

Adaptive Constant False Alarm Rate Detector Based on Long Short-term Memory Network

Chunbo XIU^{1,2}, Yifan LI^{1,2}

¹ School of Control Science and Engineering, Tiangong University, Tianjin 300387, China

² Tianjin Key Laboratory of Intelligent Control of Electrical Equipment, Tiangong University, Tianjin 300387, China

xiuchunbo@tiangong.edu.cn, yifan010409@163.com

Submitted November 11, 2024 / Accepted February 9, 2025 / Online first March 21, 2025

Abstract. *To solve the problem of degradation of detection performance of adaptive constant false alarm rate (CFAR) detectors due to low accuracy of environment recognition, an automatic clipping adaptive CFAR detector based on long short-term memory (LSTM) network is proposed. LSTM network is used to recognize the environmental type information contained in radar echo signals, and the appropriate detector is determined based on the recognition results. When there are interferences in both the leading and lagging reference windows, the interferences are clipped, and an ordered statistics CFAR detector is used to detect the target. Simulation results show that the designed adaptive CFAR detector, compared to the variability index CFAR detector, achieves an average improvement of 0.31% in detection probability in homogeneous environment. In the environment with interferences in a single-sided reference window, the average improvement in detection probability is 5.43%. In the environment with interferences in both the leading and lagging reference windows, the average improvement in detection probability is 41.57%. The automatic clipping adaptive CFAR detector based on LSTM network can more accurately recognize background environments and clipping interferences when interferences exist in both the leading and lagging reference windows, so its detection performance can be enhanced.*

Keywords

Constant false alarm rate, adaptive detection, target detection, long short-term memory network

1. Introduction

The constant false alarm rate (CFAR) detector is an essential component of radar receivers, which can adaptively set thresholds for target detection by estimating background clutter power [1–3]. Classical CFAR detectors include cell averaging CFAR (CA-CFAR) detector [4], smallest of CFAR (SO-CFAR) detector [5], greatest of CFAR (GO-CFAR) de-

tor [6], ordered statistic CFAR (OS-CFAR) detector [7], and so on. The CA-CFAR detector exhibits good detection performance in homogeneous Gaussian environments [8]. However, its performance sharply declines in interference environments, and it has a high false alarm rate in clutter edge environments [9]. The SO-CFAR detector solves the problem of degradation of target detection performance of CA-CFAR detector in the environment with interferences in a single-sided reference window. Meanwhile, the GO-CFAR detector solves the problem of high false alarm rate of CA-CFAR detector in clutter edge environment [10], [11]. However, neither of these detectors can be simultaneously applied to the environment with interferences in a single-sided reference window and clutter edge environments, and they still cannot achieve good detection results in the environment with interferences in both the leading and lagging reference windows. The OS-CFAR detector can achieve better detection performance in the environment with interferences in both the leading and lagging reference windows [12]. However, its detection performance is poor when there are multiple interferences, and it also has a high false alarm rate in clutter edge environments [13]. Therefore, the above CFAR detectors can only maintain good detection performance in a specific environment and cannot maintain stable detection performance in complex scenes with constantly changing environments. For this reason, the variability index CFAR (VI-CFAR) detector [14] determines the background type by comparing the variability index and mean ratio with their predetermined thresholds. Thus, an appropriate detector suitable for the corresponding background environment is selected, and the target detection performance in complex scenes with constantly changing environments can be enhanced. However, the VI-CFAR detector has poor detection performance when interferences in both the leading and lagging reference windows, and an increase in the number of interferences will lead to a decrease in the environmental recognition accuracy of the VI-CFAR detector, which will result in a further degradation of target detection performance [15].

To solve the problem of poor detection performance of VI-CFAR detectors in the presence of interferences in both sides of the reference window, the detection performance can

be improved by replacing the detection strategy in VI-CFAR detector. Such as, the SO-CFAR detector in the VI-CFAR detector is replaced with an S-CFAR detector in [16], and the SO-CFAR detector in VI-CFAR is replaced with an improved OS-CFAR detector in [17]. Furthermore, good environmental discrimination method can be designed to solve the problem of environmental misjudgment in VI-CFAR detectors. Such as, fuzzy theory is combined to enhance the detection performance of VI-CFAR detectors in non-homogeneous environments in [18], the robustness of VI-CFAR detectors is improved by eliminating outliers to reduce the impact of interferences on detector thresholds in [19], and the robustness of detection in multi-target environments is improved by estimating background clutter levels in [20].

Currently, the development of machine learning provides new technical support for radar constant false alarm rate (CFAR) detection [21]. Such as, target detection performance in varying environments can be improved by utilizing multilayer perceptron to adaptively select between CA-CFAR and OS-CFAR detectors [22], variability indices can be used as features to train support vector machines for environmental recognition [23], and background noise levels can be accurately estimated by utilizing convolutional neural network to remove interferences [24]. However, current commonly used detectors still cannot simultaneously show good target detection performance in environments with multiple interferences and in cluttered edge environments.

Fortunately, the efficiency of machine learning can be significantly improved by deep learning technology which can effectively solve more complex information processing problems. For instance, long short-term memory (LSTM), as a type of recurrent neural network, has shown unique performance in series data analysis [25–27]. Since radar echoes are time series data, LSTM networks can be used to improve the recognition accuracy of the environmental contained in radar echoes. Therefore, an automatic clipping adaptive CFAR detector based on long short-term memory network (ACA-LSTM-CFAR) is proposed to improve the target detection performance in different environments. LSTM networks are used to recognize noise in radar echo reference cells. When interferences exist in both the leading and lagging reference windows, the interferences are clipped, and an OS-CFAR detector is used to detect the target. The proposed detector can solve the problem of decreased detection performance in adaptive CFAR detectors due to low environmental recognition accuracy, and effectively enhance target detection performance in multi-target environments.

2. Principle of CFAR Detectors

2.1 CA-CFAR Detector

The CA-CFAR detector [4] estimates background clutter power by calculating the mean of the reference cells, and its principle of detection is shown in Fig. 1.

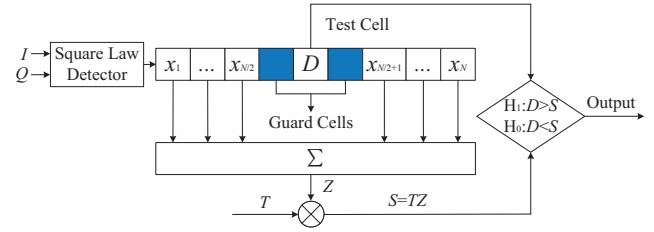


Fig. 1. Principle of CA-CFAR detector.

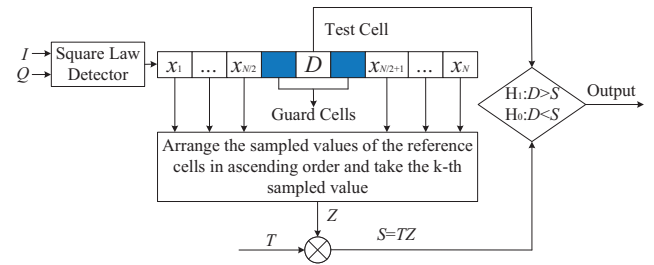


Fig. 2. Principle of OS-CFAR detector.

From Fig. 1, in the CA-CFAR detector, multiplying the estimated background noise power Z by the threshold factor T yields the detection threshold S which is compared with the power value D of the test cell to determine the detection result. When $D \geq S$, it is determined that a target exists; otherwise, it is determined that the target does not exist.

The estimated background noise power level Z is calculated as:

$$Z = \frac{\sum_{i=1}^N X_i}{N}. \quad (1)$$

The threshold factor T is determined by the length of the reference cells N and the false alarm probability P_{fa} as:

$$T = N \cdot \left(\left(P_{fa}^{-1/N} \right) - 1 \right). \quad (2)$$

The CA-CFAR detector has good detection performance in homogeneous environments but poor detection performance in interference environments and clutter edge environments [9].

2.2 OS-CFAR Detector

The OS-CFAR detector [7] estimates background clutter power by taking the k -th sampling value after ascending sorting of reference cells, and its detection principle is shown in Fig. 2.

From Fig. 2, in the OS-CFAR detector, the sampled values of the reference cells in both sides of test cell are sorted in ascending order and the k -th sampled value is selected as the estimated background noise power Z . Multiplying the estimated background noise power Z by the threshold factor T of OS-CFAR yields the detection threshold S which is compared with the power value D of the test cell to determine the detection result. When $D \geq S$, it is determined that a target exists; otherwise, it is determined that the target does not exist.

The false alarm probability P_{fa} of the OS-CFAR detector is determined by the threshold factor T , the length of the reference cells N and the k value as:

$$P_{fa} = k \binom{N}{k} \frac{\Gamma(N - k + 1 + T) \Gamma(k)}{\Gamma(N + T + 1)} \quad (3)$$

where the gamma function is defined as:

$$\Gamma(x) = \int_0^{\infty} t^{x-1} e^{-t} dt, \quad x > 0. \quad (4)$$

According to (3), the threshold factor T can be calculated by the given false alarm probability P_{fa} , length of reference cells N , and k value. Especially, the selection of k values is closely related to the accuracy of the detection results. The impact of the k value on the performance of the OS-CFAR detector is elaborated in [12]. When $k < N/2$, the false alarm probability will sharply increase in the clutter edge environment. Therefore, it is recommended to choose $k = 3/4N$ to get balanced detection performance in multi-target environments or clutter edge environments.

The OS-CFAR detector has good detection performance when there are few interferences. However, its detection performance will get poor when there are multiple interferences, and it also has a high false alarm rate in clutter edge environments [13].

2.3 VI-CFAR Detector

The VI-CFAR detector [14] can dynamically adjust the background clutter power estimation by calculating the variability index and mean ratio, and its principle of detection is shown in Fig. 3.

From Fig. 3, the variability index (VI) of the leading and lagging reference cells, and the mean ratio (MR) of all reference cells are calculated in the VI-CFAR detector.

The VI is determined by the sample variance $\hat{\sigma}^2$ and the sample mean $\hat{\mu}$ of the single-sided reference window, and it is calculated as:

$$VI = 1 + \frac{\hat{\sigma}^2}{\hat{\mu}} = 1 + \frac{1}{n-1} \cdot \frac{(\sum_{i=1}^{N/2} (X_i - \bar{X}))^2}{(\bar{X})^2}. \quad (5)$$

The MR is determined by the mean values of the leading and lagging reference window, and it is calculated as:

$$MR = \frac{\bar{X}_A}{\bar{X}_B} = \frac{\sum_{i \in A} X_i}{\sum_{i \in B} X_i}. \quad (6)$$

Comparing VI with a pre-set threshold K_{VI} can determine whether the sampling values of the reference window are homogeneous. If $VI \leq K_{VI}$, the reference window is judged to be homogeneous, otherwise, it is judged to be non-homogeneous. Comparing MR with a pre-set threshold K_{MR} can determine whether the mean values of the leading and lagging reference window are the same. If $K_{MR}^{-1} \leq MR \leq K_{MR}$, the mean values of the leading and lagging reference window are judged to be the same; otherwise, they are judged to be different. From [14], the increase in the K_{VI} and K_{MR} thresholds improves the accuracy of the judge of VI-CFAR detector in homogeneous environments, but reduces it in non-homogeneous environments. In [14], the threshold K_{VI} is recommended to be set to 4.76 and the threshold K_{MR} is recommended to be set to 1.806 to achieve better detection performance. Based on the judgment results, the appropriate detector is selected to detect the target, and the specific judgment rules are shown in Tab. 1.

In Tab. 1, T_N is the threshold factor of all reference cells, and it is calculated as:

$$T_N = (P_{fa})^{-1/N} - 1. \quad (7)$$

$T_{N/2}$ is the threshold factor of half of the reference cells, and it is calculated as:

$$T_{N/2} = (P_{fa})^{-1/(N/2)} - 1. \quad (8)$$

Although the VI-CFAR detector has a certain degree of adaptive ability, it has poor detection performance when interferences exist in both sides of the reference window, and an increase in the number of interferences will lead to a decrease in the environmental recognition accuracy of the VI-CFAR detector, which will result in a further degradation of target detection performance [15].

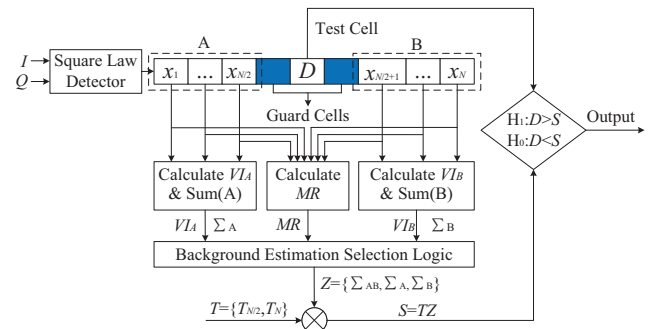


Fig. 3. Principle of VI-CFAR detector.

Leading window variable?	Lagging window variable?	Different means?	Background environment discrimination	Adaptive threshold
No	No	No	Homogeneous environment	$T_N \times (\sum(X_A) + \sum(X_B))$
No	No	Yes	Clutter edge environment	$T_N \times \max(\sum(X_A), \sum(X_B))$
Yes	No	-	Interferences in the leading window	$T_{N/2} \times \sum X_B$
No	Yes	-	Interferences in the lagging window	$T_{N/2} \times \sum X_A$
Yes	Yes	-	Interferences in the both windows	$T_N \times \min(\sum(X_A), \sum(X_B))$

Tab. 1. Adaptive threshold of VI-CFAR.

3. Improved CFAR Detectors

To solve the problem of low accuracy of environmental recognition and poor detection performance of the adaptive CFAR detector, an automatic clipping adaptive CFAR based on long short-term memory network (ACA-LSTM-CFAR) detector¹ is proposed. The long short-term memory (LSTM) network is used to improve the accuracy of environmental recognition. When interferences exist in both sides of the reference window, a clipping order statistic CFAR based on long short-term memory network (COS-LSTM-CFAR) detector is designed to improve the performance of the OS-CFAR detector by removing interferences.

3.1 ACA-LSTM-CFAR Detector

The ACA-LSTM-CFAR detector recognizes the environmental type information contained in the radar echo reference cells by LSTM network, and based on the recognition results, an appropriate detector is selected to detect the radar target. The detection principle of the ACA-LSTM-CFAR detector is shown in Fig. 4.

In Fig. 4, the in-phase signal I and quadrature signal Q received by the radar receiver are input to the ACA-LSTM-CFAR detector after passing through the square law detector. The ACA-LSTM-CFAR detector takes $N/2$ echo signals from one side of the reference window as the input and uses an interference detection module to determine whether the single-sided reference window is homogeneous. It also takes echo signals from the both sides of reference window as the input and uses a mean level detection module to determine whether the mean values of the reference windows on both sides are the same.

Both the interference detection module and the mean detection module use LSTM network for classification. The structure of the LSTM network is shown in Fig. 5.

In Fig. 5, the input layer defines the length of the input sequences and the input sequences are normalized as:

$$X_{\text{nom}} = \frac{X - X_{\min}}{X_{\max} - X_{\min}}. \quad (9)$$

The LSTM layer is used to capture long-term dependencies. The fully connected layer is used to map the output of the LSTM layer to the classification labels. The Softmax layer is used to convert the output of the fully connected layer into a probability distribution, which is calculated by Softmax function as:

$$p_i = \frac{\exp(z_i)}{\sum_{j=1}^K \exp(z_j)}. \quad (10)$$

In (10), z_i is the input element of the Softmax layer, K is the number of input elements, and p_i is the probability that the input belongs to class i .

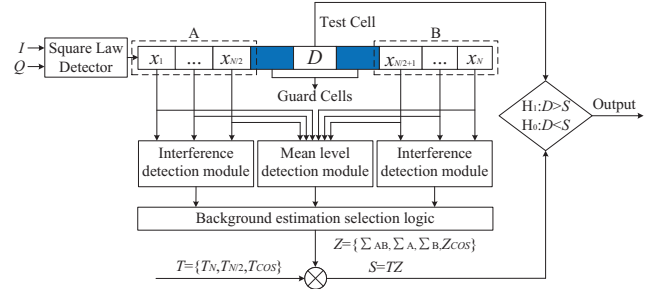


Fig. 4. Principle of ACA-LSTM-CFAR detector.

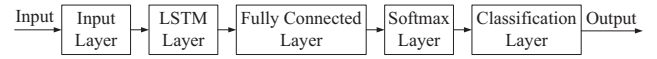


Fig. 5. LSTM classification network structure.

The classification layer is used to calculate the cross-entropy loss and generate the final classification result. When network is training, the cross-entropy loss is calculated as:

$$L = -\frac{1}{N} \sum_{i=1}^N \sum_{c=1}^C y_{i,c} \log(p_{i,c}). \quad (11)$$

In (11), L is classification error, N is the number of samples, C is the number of categories, $y_{i,c}$ is the indicator that the sample i belongs to class c , and $p_{i,c}$ is the probability of sample i being predicted as class c .

When network is predicting the final classification result is calculated as:

$$\hat{y} = \arg \max(p_i). \quad (12)$$

In (12), \hat{y} is the classification result predicted by the module. For the interference detection module, the output classification result is homogeneous environment and non-homogeneous environment. For the mean level detection module, the output classification result is homogeneous environment and clutter edge environment.

According to the classification results from the outputs of interference detection module and the mean detection module, the appropriate detector is selected for detection. The specific judgment rules are shown in Tab. 2.

In Tab. 2, T_N is the threshold factor of all reference cells, and it is calculated as:

$$T_N = (P_{\text{fa}})^{-1/N} - 1. \quad (13)$$

$T_{N/2}$ is the threshold factor of half of the reference cells, and it is calculated as:

$$T_{N/2} = (P_{\text{fa}})^{-1/(N/2)} - 1. \quad (14)$$

When both reference windows are homogeneous environments, the CA-CFAR detector is used for detection and

¹Open resource codes: <https://github.com/yifan9040/CFAR-model>.

Leading window homogeneous?	Lagging window homogeneous?	Clutter edge?	Background environment discrimination	Adaptive threshold
Yes	Yes	No	Homogeneous environment	$T_N \times (\sum(X_A) + \sum(X_B))$
Yes	Yes	Yes	Clutter edge environment	$T_N \times \max(\sum(X_A), \sum(X_B))$
No	Yes	-	Interferences in the leading window	$T_N/2 \times \sum X_B$
Yes	No	-	Interferences in the lagging window	$T_N/2 \times \sum X_A$
No	No	-	Interferences in the both windows	$T_{COS} \times Z_{COS}$

Tab. 2. Adaptive threshold of ACA-LSTM-CFAR.

takes all reference cells as input. When cluttered edge environments are detected, the CA-CFAR detector is used for detection and takes the reference cells in the higher mean value side reference window as input. When interferences exist in a single-sided reference windows, the CA-CFAR detector is used for detection and takes the reference cells in the homogeneous side reference window as input. When interferences exist in both the leading and lagging reference windows, the COS-LSTM-CFAR detector is used for detection and takes all reference cells as input.

3.2 COS-LSTM-CFAR Detector

The COS-LSTM-CFAR detector uses an LSTM network to clip interference and then uses the OS-CFAR detector for detection, thereby improving detection performance in environments with multiple interference. The detection principle of COS-LSTM-CFAR detector is shown in Fig. 6.

In Fig. 6, an interference detection module is used to independently detect both sides of the reference windows. When the interference environment is detected, the detector removes the maximum reference cell from the reference window. Then, it reuses the interference detection module to detect the reference window until the interference detection module outputs a homogeneous environment. After removing interference reference cells, the data within the reference window are sorted in ascending order. The k -th value after ascending sorting is taken as the estimated power of the background noise Z_{COS} . The estimated power of the background noise Z_{COS} is multiplied by the threshold factor T_{COS} to obtain the detection threshold S . The detection threshold S is compared with the power value of the detected cell D to obtain the detection result. When $D \geq S$, it is determined that a target exists; otherwise, it is determined that the target does not exist.

The false alarm probability P_{fa} of the COS-LSTM-CFAR detector is determined by the threshold factor T_{COS} , the length of the reference cells N , interference count i and the k value as:

$$P_{fa} = k \binom{N-i}{k} \frac{\Gamma((N-i) - k + 1 + T_{COS}) \Gamma(k)}{\Gamma((N-i) + T_{COS} + 1)}. \quad (15)$$

According to (15), the threshold factor T_{COS} can be calculated by the given false alarm probability P_{fa} , reference cell length N , interference count i , and k value.

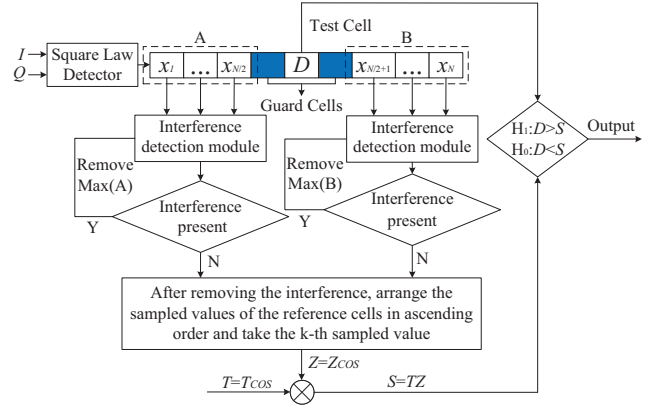


Fig. 6. Principle of COS-LSTM-CFAR detector.

4. Experiment and Result Analysis

A Monte Carlo experimental method is used to compare the environmental recognition performance of the ACA-LSTM-CFAR detector and the VI-CFAR detector. And a comparative analysis is conducted on the detection performance of various detectors, CA-CFAR detector, OS-CFAR detector, VI-CFAR detector, COS-LSTM-CFAR detector, and ACA-LSTM-CFAR detector, in different environments.

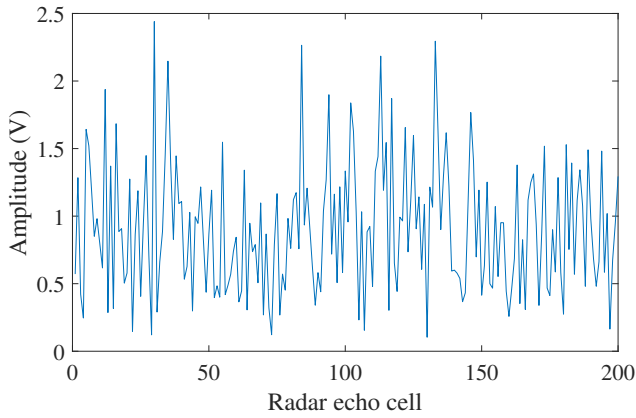
In the experiments, the number of Monte Carlo experiments for environmental recognition performance and detection performance testing are 1×10^4 , and for false alarm probability testing are 1×10^6 . The reference cell length N is 36, and the false alarm probability P_{fa} is set as 1×10^{-4} . The thresholds of the VI-CFAR detector are set as $K_{VI} = 4.76$ and $K_{MR} = 1.806$, and the k value of the OS-CFAR detector is $3/4N$ and the COS-LSTM-CFAR detector is $3/4(N-i)$.

4.1 Simulation Signal Model

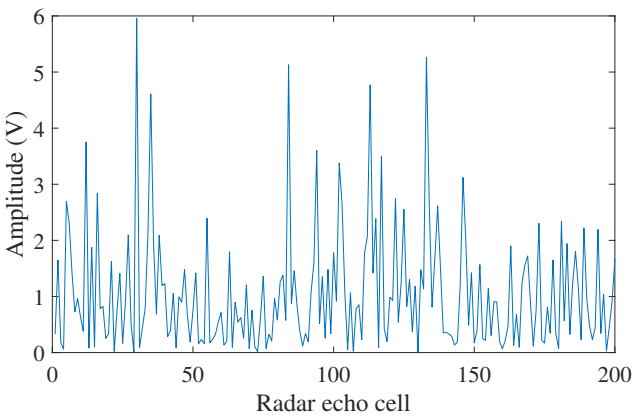
Simulated data are used in network training and Monte Carlo experiments. Under the assumption that the amplitudes of the background clutter signals I and Q follow a Rayleigh distribution, and the power of the signal passing through the square law detector follows an exponential distribution, the test cell D under H_0 has probability density function:

$$f(x|H_0) = \frac{1}{\mu} \exp\left(-\frac{x}{\mu}\right) \quad (16)$$

where μ is the scale parameter.



(a) Signals I, Q



(b) Signals passing through the square law detector

Fig. 7. Examples of radar echo signals.

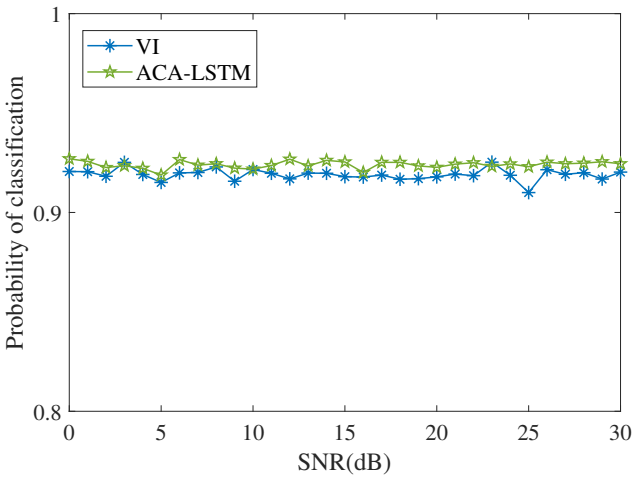


Fig. 8. Environmental recognition performances in homogeneous environments.

In a homogeneous environment, set $\mu = 1$, examples of the input signals I, Q , and the signals passing through the square law detector are shown in Fig. 7. Figure 7(a) shows that the amplitudes of the I and Q signals follow a Rayleigh distribution, while Figure 7(b) shows that the amplitude of the signals passing through the square law detector follows an exponential distribution.

Under the assumption that the target is moving fast and the radar cross section of the target changes rapidly, the target follows the Swerling II model. The test cell D under H_1 has probability density function:

$$f(x|H_1) = \frac{1}{\mu(1+S)} \exp\left[-\frac{x}{\mu(1+S)}\right] \quad (17)$$

where S is the signal-to-noise ratio. When the target exists in the reference cells instead of the test cell, it is considered as interference.

4.2 Training Data Set

Due to the different input sizes of the interference detection module and the mean level detection module, they have different training data sets. The training data set for the interference detection module consists of 4×10^4 homogeneous echo sequences and 4×10^4 echo sequences with different interferences numbers and signal-to-noise ratios. The locations of interferences is randomly generated to ensure the generalization ability of the network. And the training data set for the mean level detection module consists of 4×10^4 homogeneous echo sequences and 4×10^4 clutter edge echo sequences.

4.3 Performance Comparison of Environmental Recognition

1) Homogeneous Environment: The environmental recognition performances of the ACA-LSTM-CFAR detector and the VI-CFAR detector in homogeneous environments with signal-to-noise ratio ranging from 0 to 30 dB are shown in Fig. 8. From Fig. 8, in homogeneous environments, compared with the VI-CFAR detector, the ACA-LSTM-CFAR detector improves the recognition probability of the homogeneous environment. After calculation, the average correct recognition probability of the ACA-LSTM-CFAR detector is 92.39%, which is 0.49% higher than that of the VI-CFAR detector. Therefore, the ACA-LSTM-CFAR detector has slightly better environmental recognition performance in homogeneous environments.

2) Multiple Target Interference Environment: When interferences exist in the leading reference window and signal-to-noise ratio ranges from 0 to 30 dB, the environmental recognition performances of the ACA-LSTM-CFAR detector and the VI-CFAR detector are shown in Fig. 9. From Fig. 9, when there are four interferences in the leading reference window, compared with the VI-CFAR detector, the ACA-LSTM-CFAR detector shows a significant improvement in probability of classification at signal-to-noise ratio ranging from 0 to 20 dB. After calculation, when the signal-to-noise ratio ranges from 0 to 30 dB and there are four interferences in the leading reference window, the average correct recognition probability of ACA-LSTM-CFAR detector is 70.87%, which is 13.7% higher than that of VI-CFAR detector. Therefore, the ACA-LSTM-CFAR detector has better classification performance when there are multiple interferences in the leading reference window.

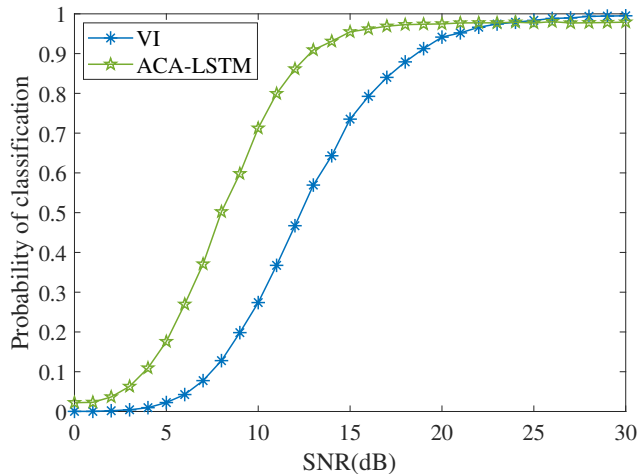


Fig. 9. Environmental recognition performances of four interferences existing in the leading reference window.

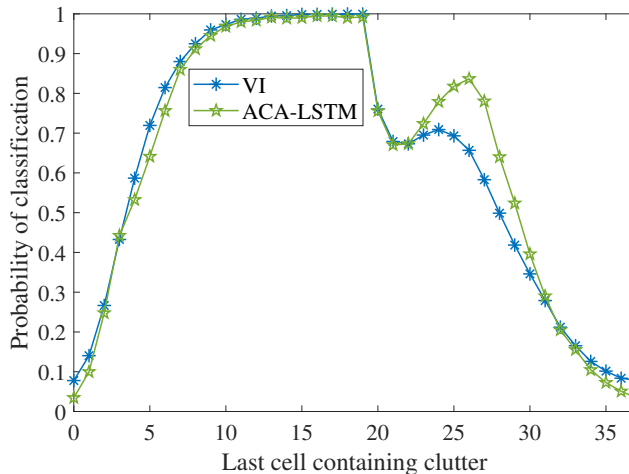


Fig. 11. Environmental recognition performances in clutter edge environment.

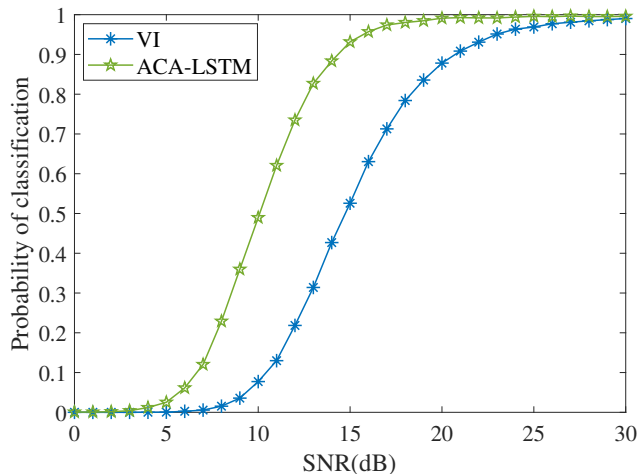


Fig. 10. Environmental recognition performances of four interferences existing in both the leading and lagging reference windows.

When interferences exist in both the leading and lagging reference windows and signal-to-noise ratio ranges from 0 to 30 dB, the environmental recognition performances of the ACA-LSTM-CFAR detector and the VI-CFAR detector are shown in Fig. 10. From Fig. 10, when there are four interferences in both the leading and lagging reference windows, compared with the VI-CFAR detector, the ACA-LSTM-CFAR detector shows a significant improvement in probability of classification at signal-to-noise ratio ranging from 5 to 25 dB. After calculation, when the signal-to-noise ratio ranges from 0 to 30 dB and there are four interferences in both the leading and lagging reference windows, the average correct recognition probability of the ACA-LSTM-CFAR detector is 64.94%, which is 15.79% higher than that of VI-CFAR detector. Therefore, the ACA-LSTM-CFAR detector exhibits better classification performance when there are multiple interferences in both the leading and lagging reference windows.

3) Clutter Edge Environment: When the background power of the weak clutter region is 1 dB and the background power of the strong clutter region is 10 dB, the environmental recognition performances of the ACA-LSTM-CFAR detector and the VI-CFAR detector in clutter edge environment are shown in Fig. 11. From Fig. 11, in clutter edge environment, compared with the VI-CFAR detector, the ACA-LSTM-CFAR detector can enhance the classification probability of clutter edge when last clutter cell between 20 and 30 cells. After calculation, the average correct recognition probability of the ACA-LSTM-CFAR detector is 62.77%, which is 0.95% higher than that of the VI-CFAR detector. Therefore, the ACA-LSTM-CFAR detector also has better classification performance in clutter edge environment.

The experimental results show that the ACA-LSTM-CFAR detector has better recognition ability than the VI-CFAR detector for homogeneous environments, multiple target interference environments, and clutter edge environments.

4.4 Comparison of Detection Performance

1) Homogeneous Environment: The detection performances of CA-CFAR detector, OS-CFAR detector, VI-CFAR detector, COS-LSTM-CFAR detector, and ACA-LSTM-CFAR detector in homogeneous environments with signal-to-noise ratio ranging from 0 to 30 dB are shown in Fig. 12. As shown in Fig. 12, in homogeneous environments, the detection performance curves of various detectors are close to the ideal curve. The detection performance of the ACA-LSTM-CFAR detector is superior to that of the VI-CFAR detector, which is superior to the COS-LSTM-CFAR detector, which is superior to the OS-CFAR detector. However, the detection performance of all four detectors is slightly lower than that of the CA-CFAR detector, and the performance of the ACA-LSTM-CFAR detector is closest to that of the CA-CFAR detector.

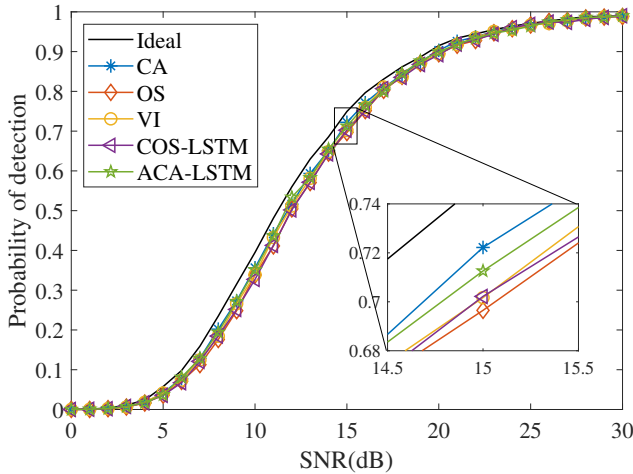


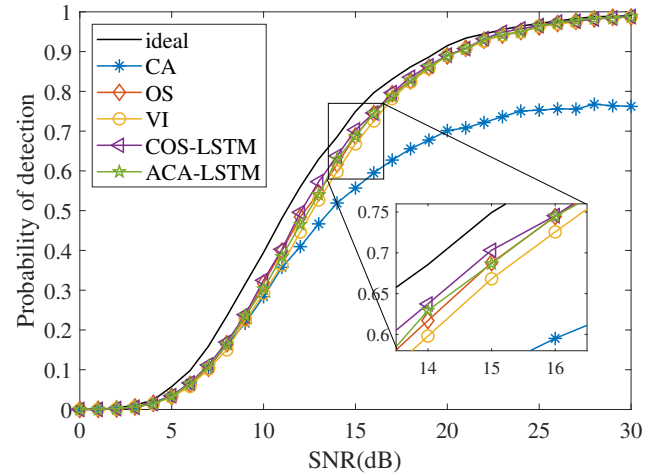
Fig. 12. Detection performances in homogeneous environments.

After calculation, in homogeneous environments with the signal-to-noise ratio ranging from 0 to 30 dB, the average detection probability of the ACA-LSTM-CFAR detector is 57.52%, which is 0.31% higher than that of the VI-CFAR detector. Therefore, the ACA-LSTM-CFAR detector exhibits better detection performance than VI-CFAR detector in a homogeneous environment.

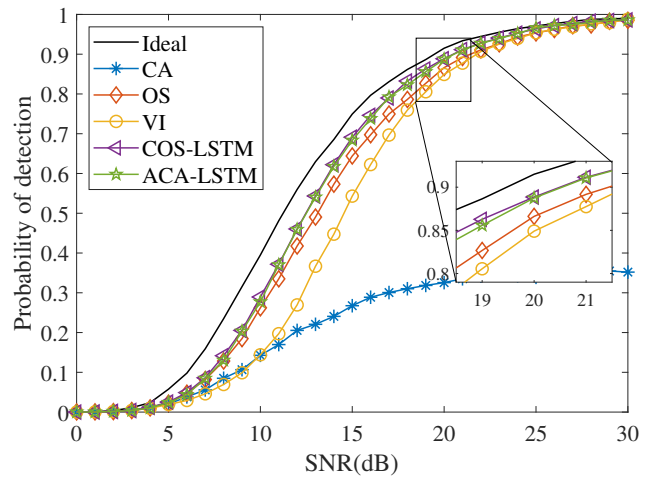
2) Multiple Target Interference Environment: When interferences exist in the leading reference window and signal-to-noise ratio ranges from 0 to 30 dB, the detection performances of the CA-CFAR detector, OS-CFAR detector, VI-CFAR detector, COS-LSTM-CFAR detector, and ACA-LSTM-CFAR detector are shown in Fig. 13. As shown in Fig. 13, when interferences exist in the leading reference window, the COS-LSTM-CFAR detector and the ACA-LSTM-CFAR detector have lower performance degradation, and can maintain a more stable detection performance as the number of interference increases.

After calculation, when there are 4 interferences in the leading reference window and the signal-to-noise ratio is 0-30dB, the average detection probability of the ACA-LSTM-CFAR detector is 55.29%, which is 5.43% higher than that of the VI-CFAR detector. Therefore, the ACA-LSTM-CFAR detector has better detection performance than the VI-CFAR detector when there is interference in the leading reference window.

When interferences exist in both the leading and lagging reference windows and the signal-to-noise ratio ranges from 0 to 30 dB, the detection performances of the CA-CFAR detector, OS-CFAR detector, VI-CFAR detector, COS-LSTM-CFAR detector, and ACA-LSTM-CFAR detector are shown in Fig. 14. As shown in Fig. 14, when interferences exist in both the leading and lagging reference windows, the COS-LSTM-CFAR detector and the ACA-LSTM-CFAR detector exhibit lower performance degradation. As the number of interferences increases, the detection performance of OS-CFAR detector decreases significantly. The COS-LSTM-CFAR detector can remove interference and maintain more



(a) Two interferences in the leading reference window



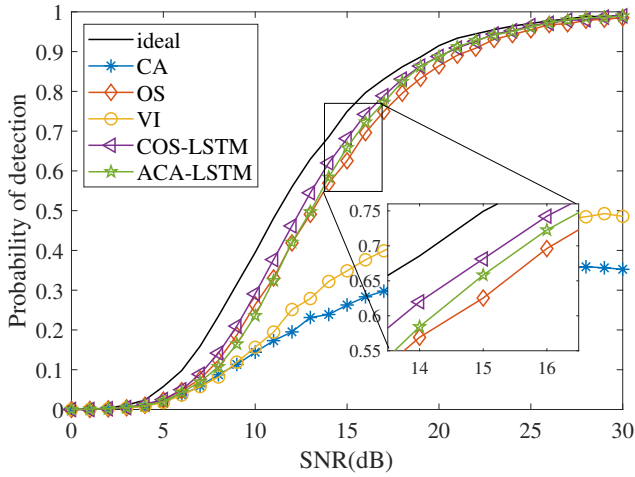
(b) Four interferences in the leading reference window

Fig. 13. Detection performances of interferences existing in the leading reference window.

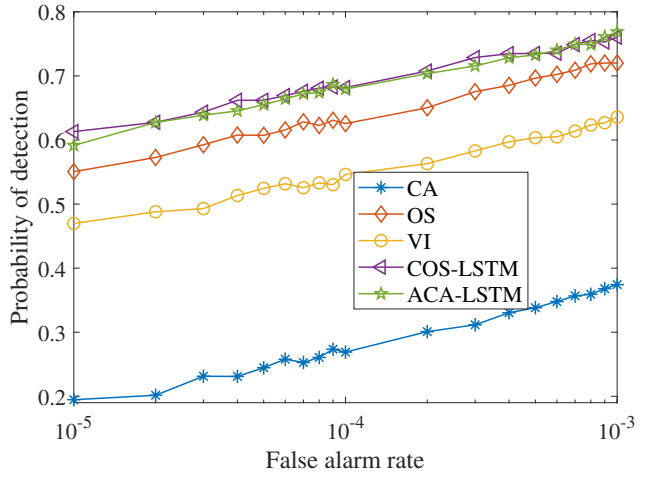
stable detection performance. However, due to the influence of environmental recognition, the detection performance of ACA-LSTM-CFAR detector is not as good as that of COS-LSTM-CFAR detector.

After calculation, when four interferences exist in both the leading and lagging reference windows and the signal-to-noise ratio ranges from 0 to 30 dB, the average detection probability of the ACA-LSTM-CFAR detector is 52.58%, which is 41.57% higher than that of the VI-CFAR detector. Therefore, the ACA-LSTM-CFAR detector has better detection performance than the VI-CFAR detector when there are interferences in both the leading and lagging reference windows.

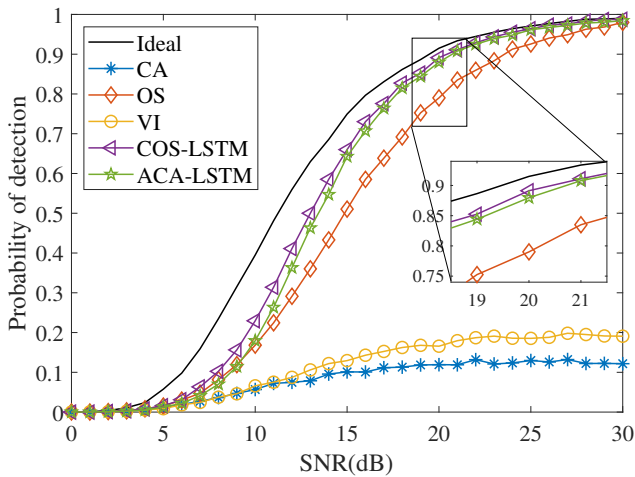
To further demonstrate the good detection performance of the proposed detector in multi-target environments with different false alarm rates, receiver operating characteristic (ROC) curves were used for comparison, where the number of interferences was 4 and the signal-to-noise ratio was 15 dB. The comparison results are shown in Fig. 15. As shown in Fig. 15, when the false alarm rate changes, the COS-LSTM-CFAR detector and the ACA-LSTM-CFAR detector still maintain better detection performance than other detectors.



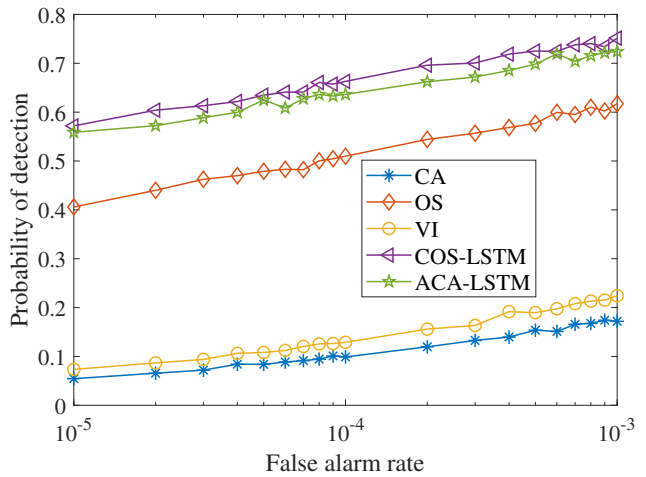
(a) Two interferences in each reference window



(a) Four interferences in the leading reference window



(b) Four interferences in each reference window



(b) Four interferences in both the leading and lagging reference windows

Fig. 14. Detection performance of interferences existing in both the leading and lagging reference windows.

Fig. 15. ROC curves in multiple target interference environment.

3) Clutter Edge Environment: When the background power of the weak clutter region is 1 dB, and the background power of the strong clutter region is 10 dB, the false alarm probabilities of the CA-CFAR detector, OS-CFAR detector, VI-CFAR detector, COS-LSTM-CFAR detector, and ACA-LSTM-CFAR detector in clutter edge environment are shown in Fig. 16. From Fig. 16, in clutter edge environments, both the VI-CFAR and the proposed ACA-LSTM-CFAR detectors can maintain good false alarm control ability. In contrast, the CA-CFAR, OS-CFAR, and COS-CFAR detectors show poorer false alarm control ability in clutter edge environments due to their lack of adaptive abilities.

After calculation, in clutter edge environments, the average false alarm probabilities of the ACA-LSTM-CFAR detector is 1.47×10^{-4} , and the average false alarm probabilities of the VI-CFAR detector is 1.34×10^{-4} . Therefore, in clutter edge environments, the false alarm probability of the ACA-LSTM-CFAR detector is close to that of the VI-CFAR detector.

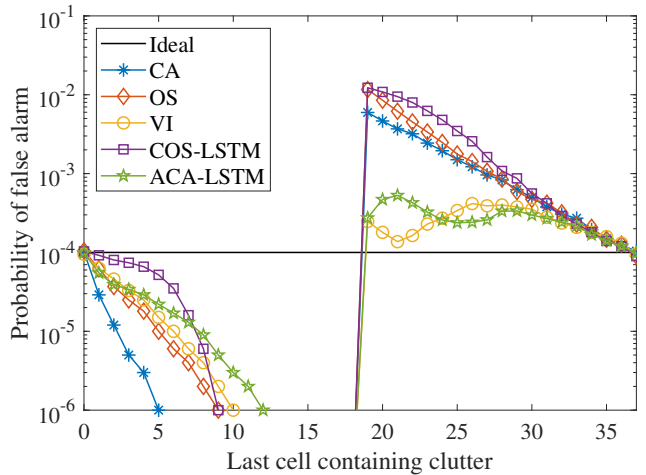


Fig. 16. False alarm probabilities in clutter edge environments.

The experimental results show that the ACA-LSTM-CFAR detector has good detection performance in homogeneous environments. In environments with multiple target interference, the detection performance of the ACA-LSTM-CFAR detector is superior to VI-CFAR and OS-CFAR detectors. Furthermore, as the number of interference increases, the ACA-LSTM-CFAR detector can maintain stable detection performance. In clutter edge environments, the COS-LSTM-CFAR detector shows poor false alarm control ability, while the ACA-LSTM-CFAR detector still shows good false alarm control ability.

5. Conclusion

A new adaptive CFAR detector based on LSTM network is proposed to improve the detection performance of radar targets. The LSTM network is used to recognize radar echo reference cell noise, and according to the recognition result, an appropriate detection algorithm is selected to detect the radar target. When interferences exist in both the leading and lagging reference windows, the interferences are clipped, and the ordered statistical constant false alarm detector is used to detect target. The environment recognition and detection performance of the ACA-LSTM-CFAR detector in various environments are tested and analyzed by Monte Carlo experiments. The simulation results show that LSTM network can more effectively recognize the environment, and when there is interference in both the leading and lagging reference windows, the background noise power level can be more accurately estimated by clipping the interference. In this way, the detection performance of the detector can be effectively improved. Furthermore, as the number of interferences increases, the detection performance of the detector will not significantly decrease. The detection probability of the proposed detector is higher than that of commonly used detectors in different environments.

References

- [1] DETOUCHE, N., LAROUCSI, T., MADJIDI, H. New log-t-based CFAR detectors for a non-homogeneous Weibull background. *Physical Communication*, 2023, vol. 59, p. 1–12. DOI: 10.1016/j.phycom.2023.102085
- [2] RIHAN, M. Y., NOSSAIR, Z. B., MUBARAK, R. I. An improved CFAR algorithm for multiple environmental conditions. *Signal, Image and Video Processing*, 2024, vol. 18, no. 4, p. 3383–3393. DOI: 10.1007/s11760-024-03001-x
- [3] LIU, X., BAI, X., WANG, D. Multi-fold high-order cumulants based CFAR detector for radar weak target detection. *Digital Signal Processing*, 2023, vol. 139, p. 1–11. DOI: 10.1016/j.dsp.2023.104076
- [4] FINN, H. M., JOHNSON, R. S. Adaptive detection mode with threshold control as a function of spatially sampled clutter-level estimates. *RCA Review*, 1968, vol. 29, p. 414–465.
- [5] TRUNK, G. V. Range resolution of targets using automatic detectors. *IEEE Transactions on Aerospace and Electronic Systems*, 1978, vol. 14, no. 5, p. 750–755. DOI: 10.1109/TAES.1978.308625
- [6] HANSEN, V. G., SAWYERS, J. H. Detectability loss due to "greatest of" selection in a cell-averaging CFAR. *IEEE Transactions on Aerospace and Electronic Systems*, 1980, vol. 16, no. 1, p. 115–118. DOI: 10.1109/TAES.1980.308885
- [7] ROHLING, H. Radar CFAR thresholding in clutter and multiple target situations. *IEEE Transactions on Aerospace and Electronic Systems*, 1983, vol. 19, no. 4, p. 608–621. DOI: 10.1109/TAES.1983.309350
- [8] WANG, X., LI, Y., ZHANG, N. A robust variability index CFAR detector for Weibull background. *IEEE Transactions on Aerospace and Electronic Systems*, 2023, vol. 59, no. 2, p. 2053–2064. DOI: 10.1109/TAES.2022.3206256
- [9] GANDHI, P. P., KASSAM, S. A. Analysis of CFAR processors in nonhomogeneous background. *IEEE Transactions on Aerospace and Electronic Systems*, 1988, vol. 24, no. 4, p. 427–445. DOI: 10.1109/7.7185
- [10] LIU, Y., ZHANG, S., SUO, J., et al. Research on a new comprehensive CFAR (Comp-CFAR) processing method. *IEEE Access*, 2019, vol. 7, p. 19401–19413. DOI: 10.1109/ACCESS.2019.2897358
- [11] XU, D., ADDABBO, P., HAO, C., et al. Adaptive strategies for clutter edge detection in radar. *Signal Processing*, 2021, vol. 186, p. 1–14. DOI: 10.1016/j.sigpro.2021.108127
- [12] SAFA, A., VERBELEN, T., KEUNINCKX, L., et al. A low-complexity radar detector outperforming OS-CFAR for indoor drone obstacle avoidance. *IEEE Journal of Selected Topics in Applied Earth Observations and Remote Sensing*, 2021, vol. 14, p. 9162–9175. DOI: 10.1109/JSTARS.2021.3107686
- [13] YANG, X., HUO, K., SU, J., et al. An anti-FOD method based on CA-CM-CFAR for MMW radar in complex clutter background. *Sensors*, 2020, vol. 20, no. 6, p. 1–20. DOI: 10.3390/s20061635
- [14] SMITH, M. E., VARSHNEY, P. K. Intelligent CFAR processor based on data variability. *IEEE Transactions on Aerospace and Electronic Systems*, 2000, vol. 18, no. 4, p. 3383–3393. DOI: 10.1109/7.869503
- [15] AI, J., MAO, Y., LUO, Q., et al. Robust CFAR ship detector based on bilateral-trimmed-statistics of complex ocean scenes in SAR imagery: A closed-form solution. *IEEE Transactions on Aerospace and Electronic Systems*, 2021, vol. 57, no. 3, p. 1872–1890. DOI: 10.1109/TAES.2021.3050654
- [16] LI, Y., JI, Z., LI, B., et al. Switching variability index based multiple strategy CFAR detector. *Journal of Systems Engineering and Electronics*, 2014, vol. 25, no. 4, p. 580–587. DOI: 10.1109/JSEE.2014.00068
- [17] QIN, T. C., WANG, Z. X., HUANG, Y., et al. VIHCEMOS-CFAR detector based on improved VI-CFAR. *Journal of Physics: Conference Series*, 2023, vol. 2613, no. 1, p. 1–12. DOI: 10.1088/1742-6596/2613/1/012007
- [18] CHEIKH, K., SOLTANI, F. Performance of the fuzzy VI-CFAR detector in non-homogeneous environments. In *Proceedings of the IEEE International Conference on Signal and Image Processing Applications (ICSIPA)*. Kuala Lumpur (Malaysia), 2011, p. 100–103. DOI: 10.1109/ICSIPA.2011.6144088
- [19] RAMAN, S. N., KALPATHI, R. R. Robust variability index CFAR for non-homogeneous background. *IET Radar, Sonar and Navigation*, 2019, vol. 13, no. 10, p. 1775–1786. DOI: 10.1049/iet-rsn.2018.5435
- [20] ZHU, X., TU, L., ZHOU, S., et al. Robust variability index CFAR detector based on Bayesian interference control. *IEEE Transactions on Aerospace and Electronic Systems*, 2022, vol. 60, p. 1–9. DOI: 10.1109/TGRS.2021.3110238
- [21] GENG, Z., YAN, H., ZHANG, J., et al. Deep-learning for radar: A survey. *IEEE Access*, 2021, vol. 9, p. 141800–141818. DOI: 10.1109/ACCESS.2021.3119561

- [22] ROHMAN, B. P. A., KURNIAWAN, D., MIFTAHUSHUDUR, M. T. Switching CA/OS CFAR using neural network for radar target detection in non-homogeneous environment. In *Proceedings of the International Electronics Symposium (IES)*. Surabaya (Indonesia), 2015, p. 280–283. DOI: 10.1109/ELECSYM.2015.7380855
- [23] WANG, L., WANG, D., HAO, C. Intelligent CFAR detector based on support vector machine. *IEEE Access*, 2017, vol. 5, p. 26965–26972. DOI: 10.1109/ACCESS.2017.2774262
- [24] LIN, C. H., LIN, Y. C., BAI, Y., et al. DL-CFAR: A novel CFAR target detection method based on deep learning. In *Proceedings of the IEEE Vehicular Technology Conference (VTC-Fall)*. Honolulu (USA), 2019, p. 1–6. DOI: 10.1109/VTCFall.2019.8891420
- [25] MOHAMMADI, F. N., MILLER, L., TAN, C. W., et al. Deep learning for time series classification and extrinsic regression: A current survey. *ACM Computing Surveys*, 2024, vol. 56, no. 9, p. 1–45. DOI: 10.1145/3649448
- [26] KARIM, F., MAJUMDAR, S., DARABI, H., et al. LSTM fully convolutional networks for time series classification. *IEEE Access*, 2018, vol. 6, p. 1662–1669. DOI: 10.1109/ACCESS.2017.2779939
- [27] KARIM, F., MAJUMDAR, S., DARABI, H., et al. Multivariate LSTM-FCNs for time series classification. *Neural Networks*, 2019, vol. 116, p. 237–245. DOI: 10.1016/j.neunet.2019.04.014

About the Authors ...

Chunbo XIU was born in Heilongjiang Province, China, received his Ph.D. degree in Navigation, Guidance and Control from Beijing Institute of Technology in 2005, and is now a Professor in the School of Control Science and Engineering at Tiangong University, where he has long been engaged in the research of artificial intelligence, radar, and robotics.

Yifan LI (Corresponding author: yifan010409@163.com) was born in Tianjin, China, received the B.S. degree in Tiangong University, is currently a master's student at Tiangong University, with a research interest in radar target detection.